



## Internal structures of a subaerial dacite cryptodome at Usu volcano, Hokkaido, Japan

メタデータ	言語: eng 出版者: 室蘭工業大学 公開日: 2007-05-16 キーワード (Ja): キーワード (En): cryptodome, dacite, subaerial, breccia, Usu volcano 作成者: 後藤, 芳彦, 伊藤, 有希恵, 横山, 由, 松井, 知之, 三松, 三郎 メールアドレス: 所属:
URL	<a href="http://hdl.handle.net/10258/59">http://hdl.handle.net/10258/59</a>

## Internal structures of a subaerial dacite cryptodome at Usu volcano, Hokkaido, Japan

著者	GOTO Yoshihiko, ITO Yukie, YOKOYAMA Yu, MATSUI Tomoyuki, MIMATSU Saburo
journal or publication title	Memoirs of the Muroran Institute of Technology
volume	54
page range	3-10
year	2004-11
URL	<a href="http://hdl.handle.net/10258/59">http://hdl.handle.net/10258/59</a>

# Internal structures of a subaerial dacite cryptodome at Usu volcano, Hokkaido, Japan

Yoshihiko GOTO \*, Yukie ITO \*, Yu YOKOYAMA \*, Tomoyuki MATSUI \*\* and Saburo MIMATSU \*\*\*

(Accepted 25 Sep 2004)

A partly eroded, subaerial, dacite cryptodome at Showa-Shinzan, Usu volcano, Hokkaido, Japan, displays its internal structures, and provides an excellent opportunity to study contact relationship between cryptodome and overlying sediment. The margin of the cryptodome comprises two facies: inner coherent dacite and outer dacite breccia. The coherent dacite facies is ~5 m in the exposed section, and consists of homogeneous or weakly flow-banded, feldspar-phyric dacite. The dacite breccia facies envelope the coherent dacite facies, and is 4-5 m thick. The breccia is monomictic, non-stratified and consists of angular dacite clasts up to 15 cm across in a cogenetic matrix. The overlying sediment directly covers the dacite breccia facies, and comprises reddish-brown, fluvial deposit. The dacite breccia formed by fracturing of coherent dacite in response to cooling contraction, and shearing of the fractured dacite due to movement of the growing cryptodome.

*Keywords:* cryptodome; dacite; subaerial; breccia; Usu volcano

---

## 1 INTRODUCTION

Silicic domes are common in felsic volcanic provinces and may be divided into two main types: lava domes and cryptodomes (McPhie et al., 1993). Lava domes are formed by extrusions of high-viscosity magma, whereas cryptodomes are high-level intrusions that cause the up doming of overlying sediments or other rocks (Minakami et al., 1951). The morphology of lava domes and different types of surface and internal structures have been described in detail and used to constrain models for dome growth (e.g., Williams, 1932; Christiansen and Lipman, 1966; Cole, 1970; Huppert et al., 1982; Fink, 1983; Fink and Manley, 1987; Swanson et al., 1987; Duffield and

Dalrymple, 1990; Swanson and Holcomb, 1990; Anderson and Fink, 1990; Dadd, 1992; Nakada, 1992; Nakada et al., 1995; Fink and Bridges, 1995). On the other hand, studies of cryptodomes are uncommon (e.g., Coats, 1936; Snyder and Fraser, 1963; Allen, 1992; Goto and McPhie, 1998; Doyle and McPhie, 2000; Stewart and McPhie, 2003) and there have been few observed events of cryptodome formation (e.g., Showa-Shinzan cryptodome, Minakami et al., 1951; Usu-Shinzan cryptodome, Katsui et al., 1985; Mount St Helens cryptodome, Lipman et al., 1981). Descriptive studies of internal structures of cryptodomes have been largely based on submarine examples in ancient successions (Goto and McPhie, 1998; Stewart and McPhie, 2003). Internal structures and contact relationships of subaerial cryptodomes in particular are poorly understood, because most modern subaerial

---

\* Department of Civil Engineering and Architecture

\*\* Date City Hall

\*\*\* Mimatsu Memorial Hall



Fig. 1. View of the Showa-Shinzan cryptodome from the west. The cryptodome still remains buried under the overlying sediment. The cryptodome mound comprises lower, platform shaped part and upper hemispherical part.

cryptodome remain buried. The 1943-1945 eruption at Usu volcano, southwestern Hokkaido, Japan, formed a subaerial dacite cryptodome, Showa-Shinzan, on the eastern foot of the volcano (Minakami et al., 1951; Mimatsu, 1995). Growth history of the cryptodome was well recorded in daily sketches from a fixed observation point, using a simple land survey instrument (“Mimatsu diagram”, Mimatsu, 1995). It is probably the best-documented example of subaerial cryptodome in the world. After 60 years, the overlying sediment of the cryptodome has been partly eroded, so that the marginal facies of the cryptodome is well exposed. The cryptodome thus provides an excellent opportunity to study internal structures of a cryptodome and contact relationship between a cryptodome and overlying sediment, as the basis for exploring underground volcanic activity during cryptodome emplacement. We have found that the margin of the cryptodome is characteristically brecciated. The objectives of this paper are: (1) to describe in detail marginal internal structures and contact of the cryptodome, (2) to determine grain-size distribution of the dacite breccia at the contact, (3) to infer forming mechanism of the dacite breccia, and (4) to compare the internal structures with those of other examples.

Because descriptive studies of subaerial cryptodomes are uncommon, some terms used to describe their internal structures require clarification. In this paper, we use ‘cryptodome’ to refer to a high-level intrusion that causes the up doming of overlying sediments or other rocks (Minakami et al., 1951; McPhie et al., 1993). The term ‘overlying sediment’ is used for sediment or rocks that existed before cryptodome intrusion but pushed up on the cryptodome due to dome emplacement. The term ‘cryptodome mound’ is used for a small mountain, which was formed by uplifting of the overlying sediment due to cryptodome emplacement. In cross section, a ‘cryptodome mound’ consists of a ‘cryptodome’ and ‘overlying sediment’.

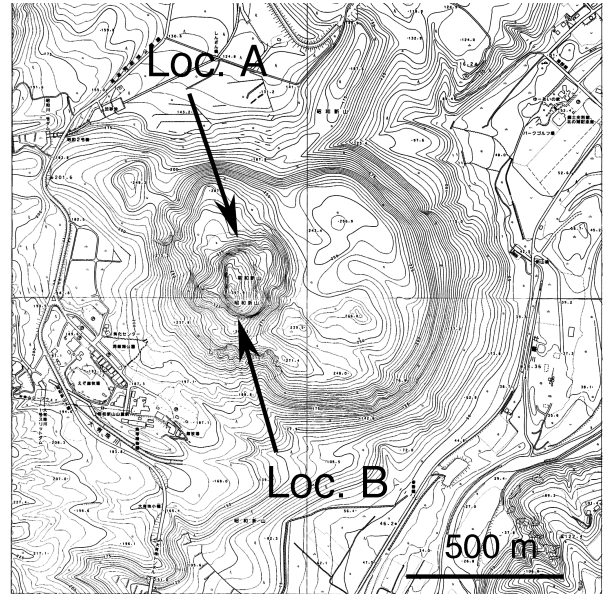


Fig. 2. Topographic map of the Showa-Shinzan cryptodome. Locations of the exposure that show contact between the cryptodome and overlying sediment (Loc. A and B) are also shown.

## 2 GEOLOGICAL SETTING

The cryptodome is a part of Usu volcano (725 m above sea level, diameter 6 km), which is located on the southern rim of the Toya Caldera. The Usu volcano comprises a stratovolcano and a number of parasitic, silicic lava domes and cryptodomes. The stratovolcano formed by eruptions of andesitic lavas (Usu somma lava) and scoria in the early Holocene age (Soya et al., 1981; Katsui et al., 1981), but its summit was broken ca. 7,000 years ago by a violent explosion, accompanied by a debris avalanche, which rushed down on the southern foot into the sea (Zenkoji debris avalanche, Soya et al., 1981). After this sector collapse, the volcano had been in a dormant state for several thousand years. The parasitic, silicic lava domes and cryptodome mounds formed in 1663, 1769, 1822, 1853, 1910, 1943-1945, 1977-1978 and 2000. They are distributed on and around the stratovolcano. The cryptodome described in this paper (i.e., the Showa-Shinzan cryptodome) formed by the 1943-1945 eruption, and is located on the eastern foot of the stratovolcano.

## 3 THE SHOWA-SHINZAN CRYPTODOME

### 3.1 Growth history

According to Minakami et al. (1951) and Mimatsu (1995), formation of the cryptodome proceeded by a series of severe earthquakes on 28 December 1943. In February 1944, the ground in the eastern foot of Usu volcano began to rise and numerous radial cracks and

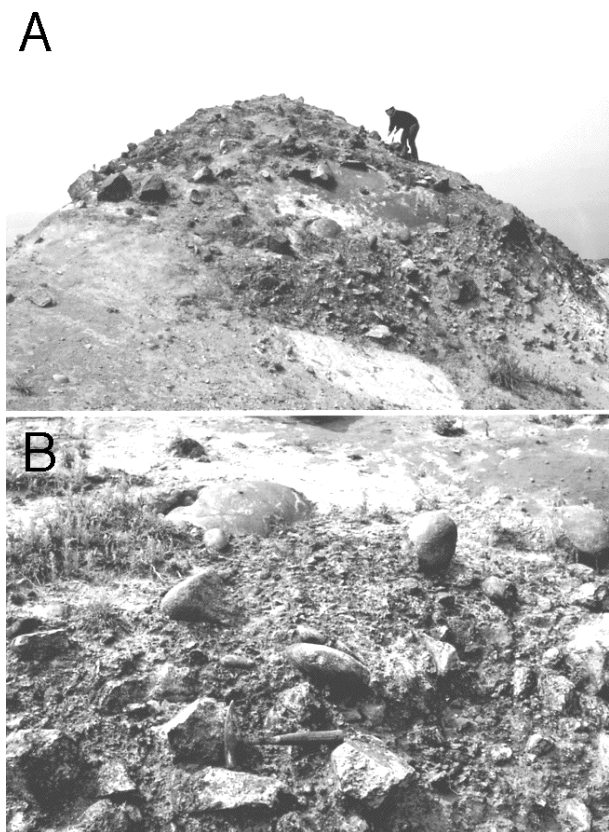


Fig. 3. (A) The summit of the cryptodome mound. It is covered with fluvial sediment. (B) Detailed view of the summit. The fluvial sediment comprises gravels in a sandy matrix.

were opened on the ground surface. The ground surface up domed continuously, and the rate of ground rise was 20-150 cm per day in June 1944. From June to October 1944, phreatic eruptions occurred on the growing cryptodome mound. The up doming of the ground surface resulted in the formation of a platform-shaped mound ("Roof mountain", Mimastu, 1995). In the middle of November 1944, the western center of the platform-shaped mound began to rise. This up rising continued at a rate of about 60 cm per day until September 1945, and formed a hemispherical projection on the platform-shaped mound. The growth of the cryptodome ceased in September 1945.

### 3.2 Morphology

The cryptodome still remains buried under the overlying sediment except for some erosion parts. The cryptodome mound is elliptical in plan view, ranging from 800 m (north - south) to 1000 m (west - east) in diameter (Fig. 1). In side view, it is 350 m thick above the surrounding area and the highest point is 398 m above sea level. The cryptodome mound comprises a lower, platform-shaped part ('Roof-Mountain', Mimastu, 1962) and a hemispherical upper part (Fig. 2b). The lower platform-shaped part is ~200 m thick above the surrounding area

and covered with overlying sediment more than 10 m thick. The upper surface of the platform-shaped part is covered with overlying sediment, more than 10 m thick. The upper, hemispherical part is ~150 m thick. Its surface is mostly (>95 %) covered with overlying sediment, but the cryptodome is partially (<5 %) exposed on erosion parts. The thickness of the overlying sediment is 5-10? m. Active fumaroles sporadically occur on this part.

### 3.3 Overlying sediment

The overlying sediment comprises fluvial deposit, pyroclastic flow deposit and andesitic lava blocks. The fluvial deposit is reddish-brown and consists of sand and andesitic gravels 5-50 cm across. The deposit originates with the alluvium distributed along Sobetsu River, which formerly flew on the flat plain where the cryptodome mound formed (Mimastu, 1995). The pyroclastic flow deposit consists of pumice up to 10 cm across and a cogenetic matrix, and is considered to be Toya pyroclastic flow deposit, which is widely distributed around Toya caldera. The fluvial deposit and pyroclastic flow deposit are highly deformed, locally intermixed, and show steep bedding along the dome morphology at the steep sides of the cryptodome. The andesitic lava blocks are 0.5-5 m across and dispersed in the fluvial deposit and pyroclastic flow deposit. The blocks consist of olivine-augite-hypersthene andesite, and probably originate with the Usu somma lava (Mimastu, 1995).

## 4 CONTACTS BETWEEN THE CRYPTODOME AND OVERLYING SEDIMENT

The contacts between the cryptodome and overlying sediment are well exposed in the vertical sections at the northern and southern parts of the cryptodome (Loc. A and B, Fig. 1).

### 4.1 Northern contact

At the northern part of the cryptodome (Loc. A, Fig. 2), the contact between the cryptodome and overlying sediment is exposed on a vertical, north-south cross section 10 m wide and 10 m high. The section comprises coherent dacite facies, dacite breccia facies and overlying sediment (Fig. 3). The coherent dacite facies is 5 m thick on the exposed section, and consists of light grey, uniform, massive dacite ( $\text{SiO}_2 = 70 \text{ wt.}\%$ , Table 1). It has irregular joints 3-15 cm apart. No columnar joints are present. The dacite is porphyritic, with 18 vol.% plagioclase phenocrysts (<1.5 mm long), 2 vol.% hypersthene phenocrysts (<1 mm long), and 1 vol.% opaque phenocrysts (<0.5 mm across). The groundmass (79 vol.%) shows an intersertal texture consisting of plagioclase microlites, quartz, cristobalite, hypersthene, opaque minerals and volcanic glass. No vesicles occur in the dacite.

The dacite breccia facies envelopes the coherent

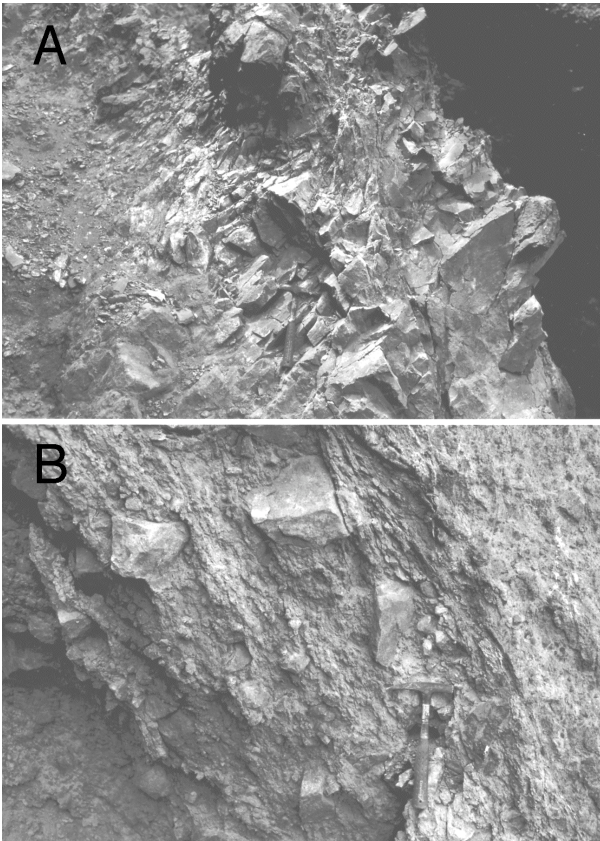


Fig. 4. (A) Coherent dacite facies at the northern contact (Loc. A). Irregular joints are developed. (B) Dacite breccia facies at the northern contact. Note that dacite clasts are embedded in a cogenetic matrix.

dacite facies and is 4-5 m thick. Boundary between the coherent dacite and the dacite breccia is distinct but gradual. The dacite breccia is non-stratified, poorly sorted, and comprises monomictic (monolithologic), angular dacite clasts up to 15 cm across in a matrix of reddish grey, cogenetic dacite fragments. The clasts are mostly clast-rotated but some near the coherent dacite (within 50 cm from the contact) shows domains of jigsaw-fit texture. The dacite of clasts has the same phenocryst assemblage, size and proportions as the coherent dacite. The matrix of the dacite breccia is composed of angular fragments of dacite, up to 5 mm across. Detailed grain-size distribution of the dacite breccia is described below. The dacite breccia facies consists only of dacite fragments and does not include fragments of overlying sediment. No peperite occurs in the dacite breccia.

The overlying sediment contacts directly with the dacite breccia facies, and is 5 m thick. Boundary between the dacite breccia and overlying sediment is sharp, and there is no mixture zone between them. The overlying sediment is a fluvial sediment. It is reddish brown, non-stratified, poorly sorted, and composed of rounded andesitic boulders and scoria in a matrix of sand. The sediment sporadically has lustrous, shear planes up to 50 cm x 100 cm wide, which have parallel

	SS-1
SiO <sub>2</sub>	70.39
TiO <sub>2</sub>	0.41
Al <sub>2</sub> O <sub>3</sub>	14.84
FeO*	3.42
MnO	0.15
MgO	0.98
CaO	3.56
Na <sub>2</sub> O	4.67
K <sub>2</sub> O	0.95
P <sub>2</sub> O <sub>5</sub>	0.14
LOI	0.48
Total	99.99

Table 1. XRF major element chemical analysis of a sample from the coherent dacite at Loc. A in Fig. 2. FeO\* = total iron as FeO; L.O.I. = loss on ignition.

striations. Each shear plane shows a different orientation of striations.

#### 4.2 Southern contact

At the southeastern part of the cryptodome (Loc. B, Fig. 2), the contact between dacite body and overlying sediment is exposed on a vertical, west-east section 25 m wide and 10 m high. The section comprises coherent dacite facies, dacite breccia facies and overlying sediment (Fig. 3).

The coherent dacite facies is 5 m thick on the exposed section, and consists of light grey, slightly flow-banded, massive dacite. The flow banding is irregular and comprises alternating dark, glassy bands 5-10 mm thick and lighter, slightly more crystalline bands up to 50 mm thick. The coherent dacite facies has irregular joints, which gradually decrease in diameter outwards from 30-100 cm at the inner part of the cryptodome to 3-20 cm at the margin of the coherent dacite facies. The dacite is porphyritic, with 18 vol.% plagioclase phenocrysts (<2 mm long), 2 vol.% hypersthene phenocrysts (<1 mm long), and 1 vol.% opaque phenocrysts (<0.5 mm across). The groundmass (79 vol.%) shows an intersertal texture consisting of plagioclase microlites, quartz, cristobalite, hypersthene, opaque minerals and volcanic glass. No vesicles occur in the dacite. The plagioclase microlites are aligned and define a flow texture that is deflected around the phenocrysts. No vesicles occur in the dacite.

The dacite breccia facies covers the coherent dacite facies and is 4-5 m thick. Boundary between the coherent dacite facies and the dacite breccia facies is gradual. The dacite breccia is non-stratified, poorly sorted and comprises monomictic (monolithologic), angular dacite clasts up to 20 cm across in a matrix of reddish grey, cogenetic dacite fragments. The clasts

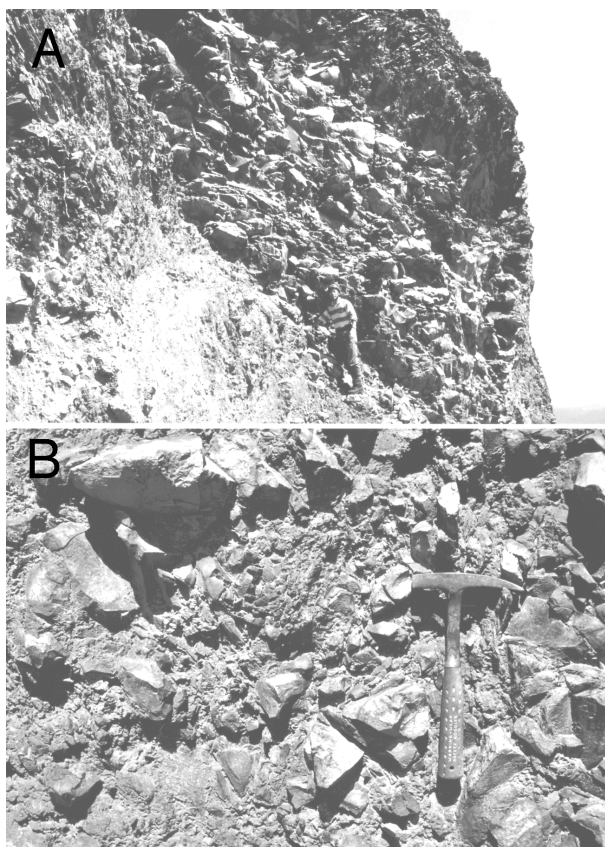


Fig. 4. Marginal facies of the cryptodome at Location B in Fig. 2. (A) Coherent dacite. Note that Irregular joints are developed, and they increase in spacing toward the centre of the cryptodome. Person for scale. (B) Dacite breccia. Note that dacite clasts are embedded in a cogenetic matrix. Hunmar for scale.

shows jigsaw-fit texture near the coherent dacite, but exhibits clast-rotated texture beyond the coherent dacite. The dacite clasts have the same phenocryst assemblage, size and proportions as the coherent dacite. The matrix of the dacite breccia is composed of angular fragments of dacite, up to 5 mm across. Grain-size distribution of the dacite breccia is described below. The dacite breccia facies consists only of dacite fragments and does not include fragments of overlying sediment. No perperite occurs in the dacite breccia.

The overlying sediment contacts directly with the dacite breccia facies, and is 5 m thick. Boundary between the dacite breccia facies and overlying sediment has been altered and not well preserved due to fumaroles. The overlying sediments consist of fluvial deposits consisting of sand and andesitic gravels 10-50 cm across. The sand is bright, reddish brown in color and indurated ('natural brick', Mimatsu, 1995). Within the sand, there are many flat, lustrous surfaces (<2 x 5 m wide) that have parallel striations. The striations are 1-2 mm deep, several millimetre intervals, and can be traced for several tens of centimeter to several metres long. The directions of striations vary in each surface.

## 5 GRAIN-SIZE DISTRIBUTION OF THE DACITE BRECCIA

Grain-size distributions were determined for the dacite breccia. The samples were collected from the dacite breccia at the northwestern (Loc. A, Fig. 2) and southwestern (Loc. B, Fig. 2) parts of the Showa-Shinzan cryptodome, and are 14.6 kg and 11.1 kg, respectively. These samples were dry sieved at 1  $\phi$  intervals (where  $\phi = -\log_2 d$ ,  $d$  being the grainsize in millimetres), using a set of sieves ranging from  $-6$  to  $5$   $\phi$  (64 to 1/32 mm). The fraction in each sieve was then weighted to 0.01 g on a laboratory balance. The results are shown in Table 2. The samples both show coarse-rich, negatively skewed, exponential grain-size distributions.

## 6 DISCUSSION

### 6.1 Formation of the dacite breccia facies

The dacite breccia facies is inferred to have formed by fragmentation of the coherent dacite facies because: (1) the breccia is monomictic (monolithologic), (2) the dacite clasts of the breccia is lithologically identical to the dacite of the coherent dacite; (3) the breccia grades into the coherent facies. The fragmentation of the coherent dacite facies may have initially caused by fracturing of coherent dacite in response to cooling contraction, because irregular joints in the coherent dacite decrease in interval outwards. The breccia beyond the coherent dacite shows clast-rotated texture, and includes very fine dacite powders between the clasts, suggesting that the breccia was formed by fracturing of dacite due to cooling contraction, and another process such as mechanical shearing. The presence of striations in both the overlying sediment and dacite breccia strongly suggests that mechanical shear occurred between the coherent dacite and overlying sediment during emplacement of the actively growing cryptodome. The striations in each domain vary in slickenside lamination direction, suggesting that the movement of the cryptodome changed in direction mincingly. The grain-size distribution of the dacite breccia is consistent to this inference. We thus infer that dacite breccia was formed fracturing of coherent dacite in response to cooling contraction, and shearing of the fractured dacite due to movement of the actively growing cryptodome.

### 6.2 Internal structures of the cryptodome

Although the exposed sections of the cryptodome are limited, the coherent facies of the exposed sections may occupy most of the central part of the cryptodome. The cryptodome is probably composed of central coherent dacite facies, which occupy most of its central part, and marginal dacite breccia facies, which cover the coherent dacite facies and is ~5 m thick. The dacite breccia facies is overlain by sediment >5 m thick.

Sample	N-1	N-1	S-1	S-1	
Location	Loc. A	Loc. A	Loc. B	Loc. B	
Size ( $\phi$ )	Size (mm)	weight (g)	weight (%)	weight (g)	weight (%)
-6	64	3351.5	22.99	3477.9	31.33
-5	32	3504.7	24.04	2301.2	20.73
-4	16	2389.5	16.39	1169.7	10.54
-3	8	1833.2	12.58	958.3	8.63
-2	4	1318.2	9.04	842.1	7.59
-1	2	857.2	5.88	673.3	6.07
0	1	515.3	3.53	440.4	3.97
1	1/2	279.1	1.91	364.3	3.28
2	1/4	196.7	1.35	250.3	2.26
3	1/8	142.7	0.98	190.1	1.71
4	1/16	89.4	0.61	147.7	1.33
5	1/32	56.3	0.39	135.6	1.22
<5	1/64	44.0	0.3	148.6	1.34
Total		14577.8	99.99	11099.5	100.00

Table 2. Grain-size distribution of the dacite breccia from Loc. A in Fig. 2 (Sample name: N-1) and Loc. B (Sample name: S-1).

According to observations during dome growth (Mimatsu, 1995), the cryptodome mound was formed by up rising of several masses. Such growth style suggests that the interior of the cryptodome consists of several lobes of dacite, like lilies bulb (Katsui, 1976). This internal structure is probably attributed to high viscosity of the dacite magma, which has high SiO<sub>2</sub> content (70 wt.%, Table 1).

The overlying sediment of the cryptodome is tilted and highly deformed, but there is no peperite at the contact, suggesting that the sediment did not fluidize by the dome emplacement. The overlying sediment has been oxidized and indurated, suggesting that the sediment was baked and solidified by the emplacement of the hot dacite magma.

### 6.3 Comparison with other examples

Descriptions of internal structures of subaerial cryptodome are very rare. Katsui et al (1988) and Kawachi (1989) described a Quaternary subaerial dacite cryptodome at Hiyori-yama, Kuttara volcano, Hokkaido, Japan, and noted that the margin of the cryptodome is highly fractured, and the overlying sediment of the cryptodome has striations. The marginal facies of the cryptodome at Hiyori-yama is probably similar to those of the Showa-Shinzan cryptodome, but details of the contact facies of the cryptodome has unfortunately not described.

Compared to rare descriptions of subaerial cryptodomes, submarine examples have been well

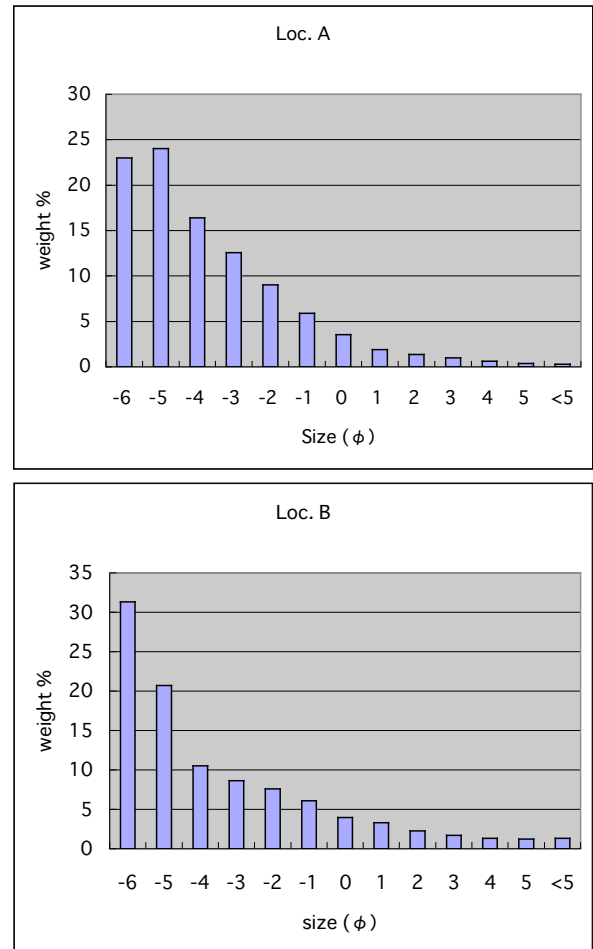


Fig. 5. Grain-size distribution of the dacite breccia at Loc. A and B.

described by several geologists (Snyder and Fraser, 1963; Goto and McPhie, 1998; Stewart and McPhie, 2003). Goto and McPhie (1998) described a Miocene submarine dacite cryptodome, 200-300 m across and 190 m high, in Hokkaido, Japan. The interior of the cryptodome comprises massive core, banded rim, and brecciated border. The brecciated border is up to 80 cm thick, and consists of in situ breccia and blocky peperite. The in situ breccia comprises polyhedral dacite clasts 5-20 cm across and a cogenetic granular matrix. The blocky peperite consists of polyhedral dacite clasts 0.5-2 cm across separated by the host sediment (mudstone). Stewart and McPhie (2003) described Pliocene submarine dacite cryptodome, exposed on the northeastern part of Milos Island, Greece. The cryptodome is 800-1300 m across and at least 120 m high. The interior of the cryptodome comprises five facies: coherent dacite facies, banded dacite facies, fractured dacite facies, massive dacite breccia facies, and the stratified dacite breccia facies.

The marginal textures of the Showa-Shinzan cryptodome resemble to those of submarine cryptodomes described above, in the presence of brecciated facies at the contact with the overlying sediment. The Showa-Shinzan cryptodome, however,

differ from those submarine examples in the absence of peprite at the contact, and presence of striations in the overlying sediment. These differences are probably attributed to degree of water saturation of the overlying sediment. In a submarine environment, the overlying sediment is water saturated and soft, so that the sediment may easily fluidize by the cryptodome emplacement. In a subaerial environment, the overlying sediment is less water saturated and harder, so that difficult to fluidize. Large friction between the cryptodome and overlying sediment may cause many striations.

## 7 CONCLUSION

A partly eroded, subaerial, dacite cryptodome at Showa-shinzan, Usu volcano, southwestern Hokkaido, Japan, shows contact relationship between cryptodome and overlying sediment. In cross section, the cryptodome comprise two facies, inner coherent dacite and outer dacite breccia. The coherent dacite facies consists of homogeneous or weakly flow-banded, feldspar-phyric dacite and has irregular joints. The dacite breccia facies envelope the coherent dacite facies, and is 4-5 m thick. The breccia is monomictic and consists of angular dacite clasts up to 15 cm across in a cogenetic matrix. The dacite breccia directly contacts with the overlying sediment, and there is no mixture zone between them. The overlying sediment is a fluvial deposit and has many striations. The dacite breccia was formed by fracturing of coherent dacite in response to cooling contraction, and shearing during dome growth. The interior of the cryptodome probably consists of large amount of coherent core and thin brecciated margin. Such internal structures closely resemble those of submarine cryptodomes, except that it has no peperite.

## ACKNOWLEDGEMENTS

K. Bull, University of Tasmania is thanked for discussions in the field. XRF analyses were performed by N. Tuchiya at Iwate University. This research was supported by Grant-in Aid for Scientific Research by Muroran Institute of Technology, Japan.

## REFERENCES

- (1) Allen, R.L., 1992. Reconstruction of the tectonic, volcanic and sedimentary setting of strongly deformed Zn-Cu massive sulfide deposits at Benambra, Victoria. *Econ. Geol.*, 87: 825-854.
- (2) Anderson, S.W., Fink, J.H., 1990. The development and distribution of surface textures at the Mount St. Helens Dome. In: Fink, J.H. (Ed.), *Lava Flows and Domes*. IAVCEI Proceedings in Volcanology 2, Springer-Verlag, Berlin, Heidelberg, pp. 25-46.
- (3) Christiansen, R.L., Lipman, P.W., 1966. Emplacement and thermal history of a rhyolite lava flow near Fortymile Canyon, southern Nevada. *Geol. Soc. Am. Bull.* 77, 671-684.
- (4) Coats, R.R., 1936. Intrusive domes of the Washoe district, Nevada. *Univ. California Geol. Sci.*, 24: 71-84.
- (5) Cole, J.W., 1970. Structure and eruptive history of the Tarawera Volcanic Complex. *N. Z. J. Geol. Geophys.* 13, 879-902.
- (6) Dadd, K.A., 1992. Structures within large volume rhyolite lava flows of the Devonian Comerong volcanics, southern Australia, and the Pleistocene Ngongotaha lava dome, N. Z. *J. Volcanol. Geotherm. Res.* 54, 33-51.
- (7) Doyle, M., McPhie, J., 2000. Facies architecture of a silicic intrusion-dominated volcanic center at Highway-Reward, Queensland, Australia. *J. Volcanol. Geotherm. Res.* 99, 79-96.
- (8) Duffield, W.A., Dalrymple, G.B., 1990. The Taylor Creek Rhyolite of New Mexico: a rapidly emplaced field of lava domes and flows. *Bull. Volcanol.* 52, 475-487.
- (9) Fink, J.H., 1983. Structure and emplacement of a rhyolite obsidian flow: Little Glass Mountain, Medicine Lake Highland, northern California. *Geol. Soc. Am. Bull.* 94, 362-380.
- (10) Fink, J.H., Bridges, N.T., 1995. Effects of eruption history and cooling rate on lava dome growth. *Bull. Volcanol.* 57, 229-239.
- (11) Fink, J.H., Manley, C.R., 1987. Pumiceous and glassy textures in rhyolite flows and implications for eruption and emplacement. *Geol. Soc. Am. Spec. Paper* 212, 77-88.
- (12) Goto, Y., McPhie, J., 1998. Endogenous growth of a Miocene dacite cryptodome, Rebun Island, Hokkaido, Japan. *J. Volcanol. Geotherm. Res.* 84, 273-286.
- (13) Huppert, H.E., Shepherd, J.B., Sigurdsson, H., Sparks, R.S.J., 1982. On lava dome growth, with application to the 1979 lava extrusion of the Soufriere of St. Vincent. *J. Volcanol. Geotherm. Res.* 14, 199-222.
- (14) Katsui, Y., Komuro, H. and Uda, T., 1985. Development of faults and growth of Usu-Shinzan cryptodome in 1977-1982 at Usu Volcano, North Japan. *Jour. Fac. Sci. Hokkaido Univ., Ser. IV.*, 21: 339-362.
- (15) Kokelaar, B.P., 1986. Magma-water interactions in subaqueous and emergent basaltic volcanism. *Bull. Volcanol.* 48, 275-289.
- (16) Lipman, P.W., Moore, J.G. and Swanson D.A., 1981. Bulging of the north flank before the May 18 eruption - geodetic data. In: P.W. Lipman and D.R. Mullineaux (Editors), *The 1980 Eruptions of Mount Saint Helens, Washington*. US Geol. Surv. Prof. Paper 1250: 143-155.
- (17) McPhie, J., Doyle, M., Allen, R., 1993. *Volcanic Textures: A Guide to the Interpretation of Textures in Volcanic Rocks*. Centre for Ore Deposit and Exploration Studies, University of Tasmania, Hobart, 198 pp.
- (18) Mimatsu, M., 1995. Showa-Shinzan Diary. Executive Committee of the 50<sup>th</sup> Anniversary of Mt. Showa-Shinzan, Sobetsu Town Office, Usu, Hokkaido, 179 pp.
- (19) Minakami, T., Ishikawa, T. and Yagi, K., 1951. The 1944 eruption of Volcano Usu in Hokkaido, Japan. *Bull. Volcanol.*, 11: 45-160.

- (20) Nakada, S., 1992. Lava domes and pyroclastic flows of the 1991-1992 eruption at Unzen Volcano. In: Yanagi, T. Okada, H., Ohta, K. (Eds.), Unzen Volcano, the 1990-1992 Eruption. The Nishinippon & Kyushu Univ. Press, pp. 56-66.
- (21) Nakada, S., Shimizu, H., Ohta, K., 1999. Overview of the 1990-1995 eruption at Unzen Volcano. *J. Volcanol. Geotherm. Res.* 89, 1-22.
- (22) Nakada, S., Miyake, Y., Sato, H., Oshima, O., Fujinawa, A., 1995. Endogenous growth of dacite dome at Unzen volcano Japan., 1993-1994. *Geology* 23, 157-160.
- (23) Snyder, G.L. and Fraser, G.D., 1963. Pillowed lavas, I: Intrusive layered lava pods and pillowed lavas Unalaska Island, Alaska. *Geol. Surv. Prof. Paper.*, 454-B: B1-23.
- (24) Soya, T., Katsui, Y., Niida, K., Sakai, K., 1981. Geological map of Usu volcano 1: 25,000. Geological map of volcanoes 2, *Geol. Surv. Jpn.*
- (25) Stewart, A.L., McPhie, J., 2003. Internal structure and emplacement of an Upper Pliocene dacitic cryptodome, Milos Island, Greece. *J. Volcanol. Geotherm. Res.* 124, 129-148.
- (26) Swanson, D.A., Holcomb, R.T., 1990. Regularities in growth of the Mount St. Helens dacite dome, 1980-1986. In: Fink, J.H. (Ed.), *Lava Flows and Domes. IAVCEI Proceedings in Volcanology 2*, Springer-Verlag, Berlin Heidelberg, pp. 3-24.
- (27) Swanson, D.A., Dzurisin, D., Holcomb, R.T., Iwatsubo, E.Y., Chadwick, W.W., Jr., Casadevall, T.J., Evert, J.W., Heliker, C.C., 1987. Growth of the lava dome at Mount St. Helens, Washington USA., 1981-1983. In: Fink, J.H. (Ed.), *The Emplacement of Silicic Domes and Lava Flows. Geol. Soc. Amer. Special Paper 212*, pp. 1-16.
- (28) Tsuchiya, N., Akanuma, H., Sakiyama, M., 1999. Major and trace element chemistry of rock samples by a popular X-ray fluorescence spectrometer using Cr anode tube. *Rept. Fac. Edu. Iwate Univ.* 59, 83-100, in Japanese.
- (29) White, J.D.L., McPhie, J., Skilling, I., 2000. Peperite: a useful genetic term. *Bull. Volcanol.* 62, 65-66.
- (30) Williams, H., 1932. The history and character of volcanic domes. *Univ. California Geol. Sci.* 21, 51-146.